J Solid State Eletrochem (2004) 8: 488–496
DOI 10.1007/s10008-003-0458-9

ORIGINAL PAPER

Enn Lust · Alar Jänes · Mati Arulepp

Influence of electrolyte characteristics on the electrochemical parameters of electrical double layer capacitors

Received: 9 July 2003 / Accepted: 19 September 2003 / Published online: 4 March 2004

Abstract Electrical double layer capacitors based on ideally polarizable nanoporous carbon electrodes in propylene carbonate with the addition of different 1 M Me_3EtNBF_4, $Me_2Et_2NBF_4$, $MeEt_3NBF_4$, Et_4NBF_4, Et_3PrNBF_4 and Et_3BuNBF_4 electrolytes have been tested by cyclic voltammetry, chronoamperometry and electrochemical impedance methods. The limits of ideal polarizability, low-frequency limiting capacitance and series resistance, time constant, Ragone plots (energy density vs. power density dependencies) and other characteristics have been discussed. The influence of the electrolyte molar mass on the electrochemical characteristics of the nanoporous carbon electrode cells has been established. The applicability limits of the Srinivasan and Weidner model have been tested.

Keywords Electrical double layer capacitor · Electrochemical impedance · Nanoporous carbon · Nonaqueous electrolytes · Tetraalkylammonium cations

Introduction

The study and modelling of the electrochemical characteristics of nanoporous carbon in different electrolyte solutions as well as electrical double layer capacitors (EDLCs) (so-called supercapacitors) is a very important problem, taking into account the development of EDLCs for high specific performances [1, 2, 3, 4, 5, 6, 7, 8, 9, 10, 11, 12, 13, 14, 15, 16]. Compared to usual dielectric capacitors, supercapacitors can supply high power during several seconds. High power density and very good cyclability make supercapacitors useful in power electronic systems and have very promising applications in many other fields of technology [1, 3, 4, 12, 13, 14, 15, 16].

A very important problem is associated with the nonaqueous electrolyte properties [1, 3, 4, 5, 6, 7, 8, 9, 10], by obtaining the characteristic relaxation frequencies, specific energy (E) and power densities (P) and other characteristics, as the specific energy density depends on the region of ideal polarizability, ΔE, of the interface between the nanoporous carbon electrode (NPCE) and the nonaqueous electrolyte solution, i.e. $E \approx (\Delta E)^2$. It should be noted that if the electrode material is electrochemically stable in the polarization region studied (ΔE), then the region of ideal polarizability is mainly governed by the electrochemical stability of the solvent and the electrolyte (i.e. salt) investigated.

The main aim of this paper is to study the influence of the electrolyte characteristics (molar mass and ion radius) on the region of ideal polarizability of the EDLCs, on the series resistance and series capacitance, on the relaxation time, on the phase angle, on the complex power and impedance and on other EDLC parameters. The electrochemical characteristics of EDLCs have been obtained with propylene carbonate (PC) as the solvent for various tetraalkylammonium tetrafluoroborate salts ($TANBF_4$). The following salts have been used as the electrolytes: Me_3EtNBF_4, $Me_2Et_2NBF_4$, $MeEt_3NBF_4$, Et_4NBF_4, Et_3PrNBF_4, Et_3BuNBF_4 ($MeEt_3NBF_4$ and Et_4NBF_4 were from Stella Chemifa, Japan; other salts were synthesized in the Institute of Organic Chemistry, Kiev, Ukraine). PC was selected because this solvent is less toxic compared with the acetonitrile (AN) widely used in EDLCs [1, 3, 4, 6, 7, 8, 9, 10].

E. Lust (✉) · A. Jänes · M. Arulepp
Institute of Physical Chemistry, University of Tartu, 2 Jakobi Street, 51014 Tartu, Estonia
E-mail: enn@chem.ut.ee
Tel.: +372-7-375165
Fax: +372-7-375160

A. Jänes · M. Arulepp
Tartu Technologies Ltd, 185 Riia Street, 51014 Tartu, Estonia

Experimental

Supercapacitor cells and measurement systems

EDLCs were built by assembling two 64.5 cm^2 electrodes between dielectric (polytetrafluoroethylene, PTFE) plates [6, 7, 8, 17, 18]. A

25-μm thick Celgard separator sheet was used between the two working electrodes. The two-electrode cells were set in a hermetic aluminium container to ensure air tightness so the cells could be tested outside the glove box. It should be noted that our assembly ensures a good tightness during many months [7, 8, 9, 10, 18, 19].

Very pure argon (99.99995%, AGA) was used for saturation of anhydrous PC stored over molecular sieves before use for the preparation of the 1 M electrolyte solutions. Impedance spectra were recorded using a Solartron frequency response analyser 1255 and potentiostat 1286 over a frequency range of 1×10^{3} to 5×10^{-3} Hz and 5 mV a.c. modulation was used. The gas phase characteristics [20] were obtained using the Gemini Sorptometer 2375 (Micromeritics) system.

Electrodes

The electrodes were made from an aluminium foil current collector and the active material layer. The active material used consisted of nanoporous carbon {prepared from TiC (H.C. Starck, grade C.A.) by the chlorination method according to the preparation scheme described elsewhere [7, 8, 9, 10, 18, 19]}, the mixture of the PTFE binder (Aldrich, 60% solution in H_2O) and carbon black (Aldrich). The carbon black was added to decrease the ohmic resistance of the electroactive material. This mixture was laminated on Ni foil and pressed together to form a very flexible layer of the active electrode material with thickness $L = 100 \pm 10$ μm. After drying and plating under vacuum, this material was covered by a very pure Al layer from one side by the vacuum spray evaporation method [7, 8, 9, 10, 18, 19]. Then the Al-covered carbon layer was spot-welded in a very pure Ar atmosphere to the Al foil current collector. The limits of ideal polarizability of Al foil have been established by cyclic voltammetry as well as by impedance spectroscopy methods [21, 22], and are wider than those for carbon electrodes.

Gas phase characteristics of the electrode material

The specific surface area, pore size distribution, micropore volume, micropore area and other parameters were measured using the Gemini Sorptometer 2375 system and calculated according to the methods described [20]. Some of the more important characteristics obtained are given in [8] and Fig. 1. According to the data in Fig. 1, the nanopores with a pore diameter $d = 0.8$–1.1 nm prevail on the carbon surface. The specific area of nanoporous carbon, obtained by the Brunauer, Emmett and Teller (BET) method, has a surface area of 1330 $m^2\ g^{-1}$. Comparison of these data with others [6, 7, 8] indicates that the specific surface area for the NPCE used in this work is somewhat higher than that for nanoporous carbon ID 711 or ID 1369, studied previously.

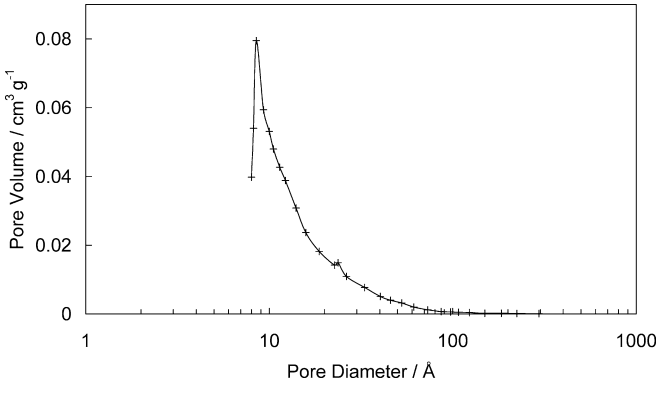

Fig. 1 Pore size distribution for nanoporous carbon

Results and discussion

Cyclic voltammetry data

The cyclic voltammograms (j vs. ΔE curves) presented in Figs. 2 and 3 show that for PC with the addition of various electrolytes the ideal capacitor behaviour has been established at potential scan rates of $v \le 10$ mV s^{-1} and at $\Delta E \le 2.5$ V (ΔE is the cell potential or voltage). At higher scan rates, distortion effects [1, 2] can be seen in the region of the potential switch-over (Fig. 3). This effect depends somewhat on the electrolyte studied and is more pronounced for salts with higher molar mass, i.e. for solutions with lower conductivity and higher viscosity. The values of the capacitance, C, can be calculated from the j vs. E curves according to Eq. 1:

$$C = I(\mathrm{d}\Delta E/\mathrm{d}t)^{-1} \tag{1}$$

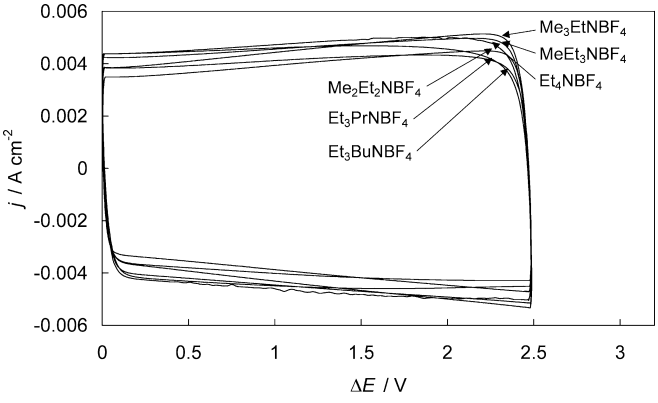

Fig. 2 Current density vs. cell potential (ΔE) curves at a potential scan rate $v = 10$ mV s^{-1} for the nanoporous carbon electrode (NPCE) cell filled with 1 M solutions of different salts in propylene carbonate (PC), noted in the figure

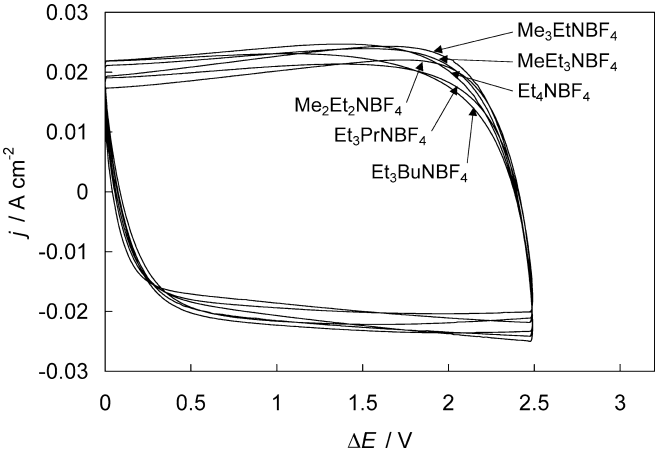

Fig. 3 Current density vs. cell potential (ΔE) curves at a potential scan rate $v = 50$ mV s^{-1} for the nanoporous carbon electrode (NPCE) cell filled with 1 M solutions of different salts in PC, noted in the figure

if we assume that the capacitance is constant and if the series resistance $R_s \to 0$ or if the current $I \to 0$ ($d\Delta E/d t = v$ is the potential scan rate). In a symmetrical (two-electrode) system, the specific capacitance C_m (farads per gram) of the activated carbon can be obtained, to a first approximation, from the capacitance of the cell by Eq. 2:

$$C_m = \frac{2C}{m} \tag{2}$$

where m is the weight (in grams) of the activated carbon. The dependence of the shape of the j vs. ΔE curves on the electrolyte, seen in Figs. 2 and 3, is mainly caused by the noticeably lower molar conductivity values of, for example, Et_3BuNBF_4 compared with Me_3EtNBF_4 in PC. Thus, Eq. 1 can be used for obtaining the capacitance values only in the region of small potential scan rates if the values of the current are very small, as the potential drop (IR drop) losses are negligible only at these conditions, and the current response is essentially that of a pure capacitor [1, 2, 7, 8, 9, 10]. Analysis of the experimental data demonstrates that for the Me_3EtNBF_4|NPCE interface, the values of C somewhat increase with ΔE and are practically independent of v if $v \le 10$ mV s^{-1}. The same is valid for the $Me_2Et_2NBF_4$, Et_3MeNBF_4 and Et_4NBF_4 salts. For the PC + Et_3BuNBF_4 interface, the values of C are practically independent of ΔE if $\Delta E \le 1.5$ V. At $\Delta E \ge 2.0$ V, C starts to decrease, which is caused by the repulsion interaction between the adsorbed Et_3BuN^+ ions at the negatively charged electrode because the capacitance values for the negatively charged electrode are somewhat lower than for the positively charged electrode where the BF_4^- anion adsorption takes place [7, 8]. The more expressed repulsion interaction between the adsorbed Et_3BuN^+ cations compared with Me_3EtN^+ cations is mainly caused by the higher molar volume, i.e. by the larger virial surface area engaged by an adsorbed cation [1, 23]. Thus, the nearly equilibrium values of the capacitance can be obtained only at slow potential scan rates and at $\Delta E \le 2.0$ V for all electrolytes studied. The lower values of C for Et_3BuNBF_4 at $\Delta E > 2.0$ V and $v \ge 5$ mV s^{-1} are mainly caused by the deviation of the system from the ideally polarizable electrode (discussed in more detail later).

Electrochemical impedance data

According to the data in Fig. 4, the complex plane plots {Nyquist plots, where $Z'' = (j\omega C_s)^{-1}$ is the imaginary part of impedance, $\omega = 2\pi f$ is the angular frequency and $Z'(\omega \to \infty) = R_s$ is the real part of the impedance [1, 23, 24, 25, 26, 27, 28, 29, 30, 31, 32]} for all salts studied, demonstrate fairly conventional behaviour for a porous electrode system with a uniformly distributed solution resistance R_s (Fig. 5) and a double layer series capacitance C_s is exhibited with a phase angle value $|\delta| \le 45°$ for an a.c. frequency $0.03 < f < 100$ Hz (usually called the

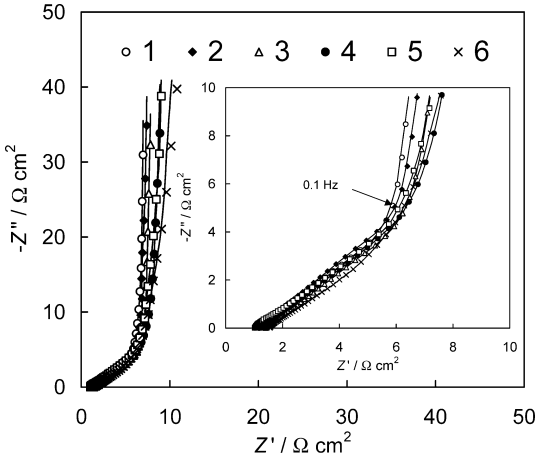

Fig. 4 Complex plane plots for the NPCE cell filled with 1 M solutions of different salts in PC at $\Delta E = 2.5$ V (*1*, Me_3EtNBF_4; *2*, $Me_2Et_2NBF_4$; *3*, $MeEt_3NBF_4$; *4*, Et_4NBF_4; *5*, Et_3PrNBF_4; *6*, Et_3BuNBF_4). *Solid lines*: fitting according to the Srinivasan and Weidner model [5, 30]

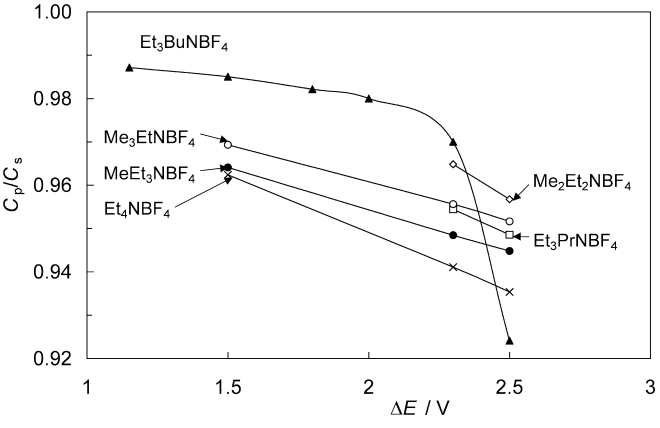

Fig. 5 The ratio C_p/C_s vs. ΔE plots for the NPCE cell filled with 1 M solutions of different salts in PC, noted in the figure

nanoporous section of the complex plane plot) [1, 2, 3, 4, 5, 6, 7, 8, 9, 10]. Extrapolation of the high-frequency part of the Z'' vs. Z' curve in Fig. 4 to the condition $Z'' = 0$ gives the equivalent series resistance (ESR) of the cell (R_E), i.e. $R_E = Z'(\omega \to \infty) = R_s(\omega \to \infty)$. According to the data in Fig. 4, R_E increases in the order of the salts $Me_3EtNBF_4 < Et_4NBF_4 < Et_3BuNBF_4$, i.e. with decreasing molar conductivity of the electrolyte in the NPCE cell (i.e. with increasing molar mass of the cation studied) [33, 34]. Comparison of the data for various electrolytes at different ΔE values shows that for Me_3EtNBF_4 there is only a very weak dependence of R_E on ΔE and only at $\Delta E \ge 2.7$ V does R_E somewhat increase with increasing ΔE. For Et_3BuNBF_4 solution, the dependence of R_E on ΔE is comparatively high. This result indicates that the values for R_E are determined not only by the series resistance of the electrolyte (and electrode material and other contact resistance values) [1, 2, 3, 4, 5, 6, 7, 8, 9, 10], but R_E is a very complicated

function of the NPCE|electrolyte interface structural parameters, i.e. of the electrolyte matrix conductivity (i.e. conductivity of the electrolyte solution in the nanopores), as well as of the very slow (probably faradaic) processes occurring at the NPCE|Et_3BuNBF_4 solution interface at higher ΔE.

The finite length effects (i.e. the knee in the Z'' vs. Z' plots) [1, 5, 23, 30, 31, 32] at very low frequencies ($f \leq 0.1$ Hz) has been established. It should be noted that there are two possible finite length effects for porous electrodes [5, 23, 30, 31, 32]. A knee or kink in the Nyquist plot can occur for a porous electrode connected with a double layer closing only as a consequence of the field penetration into the pores. For higher frequencies the Nyquist impedance corresponds to Warburg-like impedance, depending on the double layer capacity and on the electrolyte resistance inside the pores [31]. On decreasing the a.c. frequency down from a certain characteristic frequency value, the penetration of the pores is complete and the electrode behaviour is similar to an ideal capacitor [5, 31]. However, a kink in the Nyquist plot can occur if the diffusion wavelength is comparable to the thickness of a finite diffusion region corresponding to the finite length bulk diffusion for reflective boundary conditions [5, 32]. As shown by Srinivasan and Weidner [5], differentiating between these two processes based on a Nyquist plot as above is not possible. Extrapolation of these nearly linear parts of the Z'' vs. Z' plot in Fig. 4 to the condition $Z'' = 0$ gives the sum (R_Σ) of the ESR (R_E) and the internal distribution of the electrolyte resistance values (R_{IER}) in the pore matrix of the EDLC, usually called the distributed pore resistance (R_{pore}), i.e. $R_\Sigma = R_E + R_{pore}$. The a.c. response of the EDLC filled with PC + Me_3EtNBF_4 electrolyte shows only a very weak dependence of R_{pore} on the potential difference applied if $\Delta E < 2.0$ V, but R_{pore} increases noticeably with ΔE at $\Delta E > 2.5$ V. For the PC + Et_3BuNBF_4 electrolyte cell, the values of R_E and R_{pore} depend noticeably on ΔE, in agreement with the dependence of the phase angle on ΔE obtained at low frequencies.

According to the experimental data (Fig. 4), the deviation of the PC + Et_3BuNBF_4|NPCE interface from the purely adsorption limited stage (ideal capacitive behaviour) increases with ΔE, but these deviations are comparatively small for the Me_3EtNBF_4 and $Me_2Et_2NBF_4$ salts in PC. Differently from the data for AN solutions [6, 7, 8], where the very wide plateaus at $f < 5\times10^{-2}$ Hz with a phase angle $|\delta| \geq 85°$ have been obtained, the absolute values of δ for PC are noticeably lower than $|\delta| \leq 80°$. This result is in good agreement with the data in Fig. 5, where the dependence of the ratio of the parallel capacitance, C_p, to the series capacitance, C_s, on ΔE is shown. The values of C_p/C_s are somewhat lower than 1.0 ($C_p/C_s = 1.0$ corresponds to the ideally polarizable electrochemical system [23, 24, 25, 26, 27, 28, 29, 30, 31, 32]), and the inversely proportional dependence of C_p/C_s on ΔE indicates the deviation of the NPCE|electrolyte interface from the ideally polarizable electrochemical system. At $0.1 < f < 10$ Hz for all electrolytes studied, the very short second plateau with $\delta = -45°$ has been observed. The value of the frequency corresponding to the phase angle $\delta = -45°$ defines the supercapacitor relaxation time constant, $\tau_R = (2\pi f_R)^{-1}$. At times shorter than τ_R, the series capacitance established, $C_s(\omega)$, is lower than half of the low-frequency series capacitance $C_s(\omega \to 0)$ [1, 2, 3, 4, 5, 12, 13, 14, 15]. It should be mentioned that at low frequencies ($f < 0.1$ Hz) the phase angle values are practically independent of electrolyte (i.e. salt cation) studied and, thus, at very low frequencies the time-dependent (i.e. relaxation) characteristics of the NPCE|PC + salt system are mainly determined by the solvent (i.e. PC) characteristics [6, 7, 8].

According to the experimental data in Fig. 6, the series capacitance at $\omega \to 0$ [$C_s(\omega \to 0)$] for the NPCE|Me_3EtNBF_4, $Me_2Et_2NBF_4$, $MeEt_3NBF_4$ or the Et_4NBF_4 + PC interface depends nearly linearly on ΔE, but for the Et_3BuNBF_4 + PC electrolyte a more complicated dependence has been observed. It was found that at $\Delta E > 2.0$ V (Fig. 5) there is no purely adsorption-limited stage at $\omega \to 0$ and, at $\Delta E > 2.0$ V, C_s as well as C_p begins to decrease (Fig. 6). At higher frequency, the C_s and C_p values strongly depend on f (i.e. on the a.c. penetration length) for all electrolytes studied, and, at fixed $f \geq 1$ Hz, C_s is practically independent of the TAN^+ studied. At $0.005 < f < 0.1$ Hz the slope of the C_s vs. $\log f$ plot as well as the C_p vs. $\log f$ plot noticeably depend on the electrolyte characteristics. At $f \leq 0.01$ Hz, the values of C_s (and C_p) for the Me_3EtNBF_4 + PC|NPCE interface are 20–25% higher than those for the Et_3BuNBF_4 or Et_3PrNBF_4 + PC electrolyte. Differently from the Me_3EtNBF_4, $Me_2Et_2NBF_4$, $MeEt_3NBF_4$ and Et_4NBF_4 electrolytes, the noticeable frequency dependence of C_s and C_p at $f \leq 0.01$ Hz indicates that the adsorption equilibrium in the whole porous electrode matrix is not reached for the Et_3BuNBF_4 or for the Et_3PrNBF_4 electrolytes even at $f \leq 5\times10^{-3}$ Hz. This is mainly caused by the lower effective diffusion coefficient values for the larger cations in the NPCE.

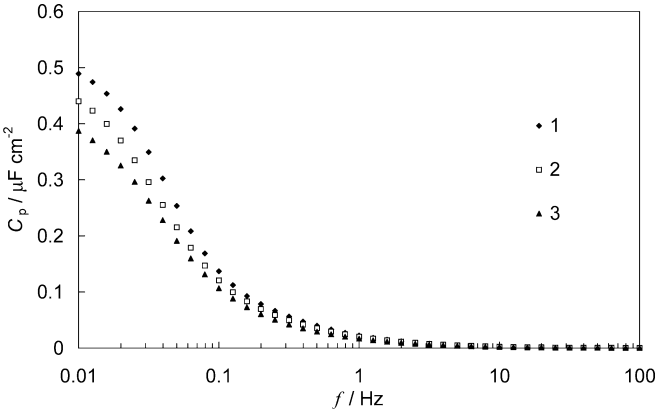

Fig. 6 Parallel capacitance vs. frequency plots for the NPCE cell filled with 1 M solutions of different salts in PC at $\Delta E = 2.5$ V (*1*, Me_3EtNBF_4; *2*, Et_4NBF_4; *3*, Et_3BuNBF_4)

The crossing of the middle-frequency part of the Z'' vs. Z' plot with the low-frequency nearly vertical part (Fig. 4) (nearly capacitive behaviour with the heterogeneous adsorption-limited stage) defines the "knee frequency" f^0 ($\omega^0 = 2\pi f^0$). Below this frequency the whole capacitance is mainly reached to establish a finite value for the Me_3EtNBF_4 and $Me_2Et_2NBF_4$ + PC solutions (Fig. 6). According to the experimental data, ω^0 is practically independent of electrolyte studied, but ω^0 somewhat decreases with increasing ΔE. The small decrease of ω^0 with increasing ΔE is probably mainly caused by the electrolyte starvation effect [1, 2, 6, 7, 8, 10]. This behaviour can arise because a significant fraction of the otherwise free conducting ions of the electrolyte become electrostatically adsorbed in the distributed double layer and, thus, diminish the conductivity of the accompanying "free" electrolyte and a longer time is needed to establish the adsorption equilibrium between the solution base and the NPCE surface. For electrolytes with higher molar mass (i.e. for Et_3PrNBF_4 and Et_3BuNBF_4 with larger molar volumes), with the rise of ΔE the limiting Gibbs adsorption of the adsorbed ions will be established at lower frequencies than 5×10^{-3} Hz. These conclusions are in very good agreement with the parallel capacitance C_p vs. frequency plots (Figs. 5 and 6). It should be noted that, for the PC|NPCE interface, a noticeable dependence of the low-frequency series resistance $R_s(\omega \to 0)$ as well as $R_p(\omega \to 0)$ on the TAN^+ molar mass has been established, increasing with ΔE. The comparatively moderate parallel resistance R_p values for the PC + electrolyte system probably show the very slow rate of the faradaic processes, increasing only somewhat with ΔE at $\Delta E \geq 2.5$ V.

The values of the real part $C'(\omega)$ and imaginary part $C''(\omega)$ of the capacitance have been calculated according to following equations:

$$C_S(\omega) = C'(\omega) - jC''(\omega) \tag{3}$$

$$C'(\omega) = -\frac{Z''(\omega)}{\omega|Z(\omega)|^2}; \qquad C''(\omega) = \frac{Z'(\omega)}{\omega|Z(\omega)|^2} \tag{4}$$

where $Z(\omega)$ is the complex impedance [3]. It should be noted that the low-frequency part of $C'(\omega)$ for the NPCE cell corresponds to the static capacitance, which is measured during the constant current discharge (or calculated from i vs. ΔE curves measured at very slow potential scan rates) [1, 2, 3, 4, 5, 6]. The imaginary component of the capacitance $C''(\omega)$ corresponds to the energy dissipation of the capacitance $C_s(\omega)$, i.e. it corresponds to the energy dissipation by an irreversible process which can lead to the hysteresis of the electrochemical processes [1, 3]. It was found that the values of $C'(\omega)$ obtained are in the excellent agreement with the values of $C_p(\omega)$ calculated using the classical calculation scheme [26, 27, 28, 29, 30, 31].

According to the results in Fig. 7, the C'' vs. f dependences have a maximum at the relaxation frequency f_R, determining the time constant $\tau_R = (2\pi f_R)^{-1}$ (Fig. 7). Analysis of the data in Figs. 5, 6, 7 shows that only half of the low-frequency capacitance is reached at τ_R [2, 3]. It should be noted that according to published ideas [1, 3], this time constant has been described as a dielectric relaxation time and as a supercapacitor factor of merit [1, 15]. According to the experimental results at moderate ΔE values, τ_R is practically independent of electrolyte and ΔE if $\Delta E \leq 2.0$ V. At $\Delta E \geq 2.0$ V, τ_R begins to increase (Fig. 7) and C'' depends on the TAN^+ cation studied. Comparison of our data with other data [3] shows that the values of τ_R are lower for the NPCE capacitors than for a cell prepared from PICACTIF SC produced by the Pica Company [3]. Thus, the ideal capacitive behaviour for the NPCE|PC + Et_4NBF_4 electrolyte interface will be established at higher frequencies compared with the PICACTIF SC|PC + Et_4NBF_4 interface.

Complex power plots

The values of the complex power can be expressed as [3]:

$$S(\omega) = P(\omega) + jQ(\omega) \tag{5}$$

where the real part of the power is:

$$P(\omega) = \omega C''(\omega)|\Delta V_{rms}|^2 \tag{6}$$

and the imaginary part of the power is:

$$Q(\omega) = -\omega C'(\omega)|\Delta V_{rms}|^2 \tag{7}$$

with $|\Delta V_{rms}|^2 = \Delta V_{max}/\sqrt{2}$ (V_{max} is the maximal amplitude of the a.c. voltage). An ideal capacitor (i.e. a system with ideal capacitive behaviour) has no real part, as there is only the reactive contribution to the complex power, and Eq. 5 simplifies to:

$$S(\omega) = jQ = -\frac{j\Delta V_{rms}^2}{|Z''|} = -j\omega C \Delta V_{rms}^2 \tag{8}$$

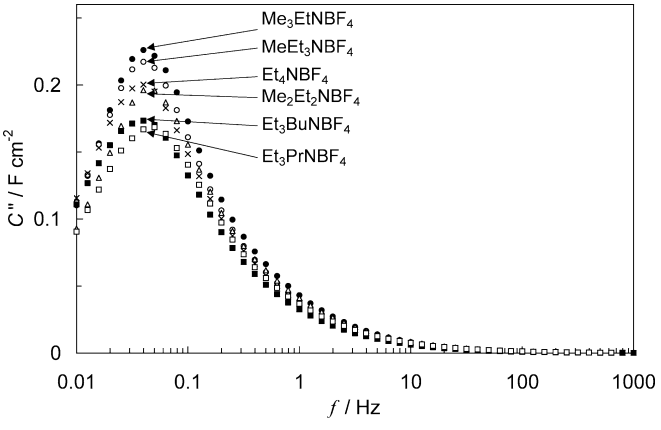

Fig. 7 Dependence of the imaginary part of capacitance on frequency for the NPCE cell at $\Delta E = 2.5$ V, filled with 1 M solutions of different salts in PC, noted in the figure

Systems with an ideal resistive behaviour (ideal resistance) have no imaginary part as this component only dissipates energy and the complex power takes the well-known form [3]:

$$S(\omega) = \frac{|\Delta V_{\mathrm{rms}}|^2}{|Z'|} \tag{9}$$

It should be noted that real EDLCs oscillate between the two states mentioned previously: a resistive one at high frequencies ($\omega \to \infty$) and a nearly capacitive one at low frequencies ($\omega \to 0$). Between these two states, EDLCs behave like a resistance-capacitance (RC) transmission circuit. The dependence of the normalized real part ($P(\omega)/|S|$) and the imaginary part ($Q(\omega)/|S|$) for the complex power are presented in Fig. 8. In good agreement with the data in Fig. 7, the relaxation time constant τ_{R}, obtained as the frequency of the intersection point of the ($P(\omega)/|S|$) vs. log f and ($Q(\omega)/|S|$) vs. log f plots, is practically independent of the electrolyte cation used. However, the results for the same salt in different solvents demonstrated a very noticeable dependence of τ_{R} on the solvent viscosity, dielectric permittivity and dipole moment [10]. Thus, according to these data and the data in Figs. 7 and 8, the low-frequency behaviour of the NPCE|PC + electrolyte interface is mainly determined by the solvent characteristics. Thus, comparison of the data for the cells filled with various electrolytes (salts) [6, 7, 8] indicates the huge influence of the molar conductivity (i.e. viscosity of various solvents) and a very small influence of the salt characteristics on the low-frequency characteristics of the NPCE|nonaqueous electrolyte interface if the same solvent is used.

The dependences of the real (ϵ') and imaginary (ϵ'') parts of the complex dielectric constant on the frequency at fixed ΔE are in good agreement with the complex power data. According to the experimental data, ϵ' is practically independent of ΔE, but ϵ' somewhat increases with decreasing molar mass (molar volume) of the TAN^+ cation studied [33, 34]. However, this effect is noticeable only at very low frequencies, i.e. in the region of the limiting static dielectric constant values [1, 23]. In the region of high frequency the limiting dielectric constant values $\epsilon' \to \epsilon_\infty$ are independent of ΔE as well as of the TAN^+ cation characteristics. A minimum in the ϵ'' vs. log f dependence and the depth of this minimum is inversely proportional to the molar mass of the TAN^+ cation studied and the frequency of this minimum ($f_{\mathrm{min}} = 0.04$ Hz at $\Delta E =$ constant is practically independent of cation as well as ΔE if the same salt is investigated). The depth of the minimum in the ϵ'' vs. log f plots only weakly decreases with increasing ΔE if $\Delta E \leq 2.0$ V, i.e. as the rate of the faradaic processes increases.

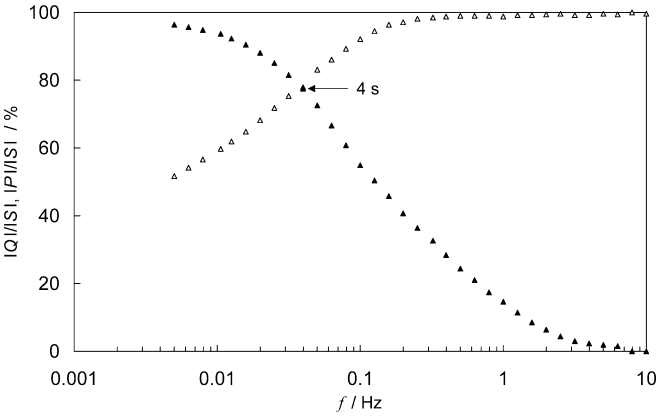

Fig. 8 Normalized reactive power $|Q|/|S|$ (*open symbols*) and active power $|P|/|S|$ (*filled symbols*) vs. frequency plots for the NPCE cell filled with 1 M solutions of $MeEt_3NBF_4$ in PC at $\Delta E = 2.5$ V

Fitting the complex plane plots for NPCE capacitors

For a more detailed characterization of the EDLCs based on the NPCE, the model developed by Srinivasan and Weidner [5] (SWM) has been used. In this model it was assumed that the cell consists of two identical porous electrodes [31] with a separator between them and an electrolyte throughout. It was assumed that (1) all faradaic processes result in a current–voltage profile similar to that of a capacitor; (2) the electrolyte concentration is uniform throughout; (3) ohmic losses are the dominating phenomena behind the heating effect; (4) the temperature is constant throughout the cell; (5) the capacitance is constant over the voltage window of the operation; and (6) the physical properties of the device (e.g. conductivity and capacitance) do not vary during a charge (or discharge). According to the SWM theory, the dimensionless complex impedance $Z^*(\omega^*)$ is obtained as:

$$Z*(\omega) = \mathrm{Re}*(\omega*) + j\mathrm{Im}^*(\omega*) \tag{10}$$

where $\mathrm{Re}^*(\omega^*)$ and $\mathrm{Im}^*(\omega^*)$ are the dimensionless real and imaginary parts of the impedance and ω^* is the dimensionless frequency [5]. The equations for the real and imaginary parts of the impedance are given in [5] and, according to the SWM theory, the impedance of an electrochemical capacitor is a function of ω^* as well as of two other dimensionless parameters, i.e. of β (the ratio of the external to the internal resistance, $\beta = R_{\mathrm{E}}/R_{\mathrm{IER}}$) and y (the ratio of the effective solution conductivity to the matrix phase conductivity, $y = \kappa/\sigma$).

For the simulation of the experimental Z'' vs. Z' plots, the complex impedance is expressed as [5, 30]:

$$Z(\omega) = R'\left[\frac{4(\kappa/\sigma)}{[1+(\kappa/\sigma)]^2\sqrt{j\omega t}\sinh(\sqrt{j\omega t})} + \frac{2\left[1+(\kappa/\sigma)^2\right]}{[1+(\kappa/\sigma)]^2}\frac{\coth(\sqrt{j\omega t})}{\sqrt{j\omega t}} + \frac{2(\kappa/\sigma)}{[1+(\kappa/\sigma)]^2}\right] + R_{\mathrm{sep}} \tag{11}$$

where:

$$R' = \frac{L(\kappa + \sigma)}{S\kappa\sigma} \tag{12}$$

and R_{sep} is the resistance of the electrolyte in the separator, obtained as $R_{sep} = L_s/S_s\kappa_s$ (L_s is the separator thickness, κ_s is the effective conductivity of the electrolyte in the separator, and S_s is the flat cross-section area of the separator); L is the electrode thickness, κ and σ are the effective conductivities of the electrolyte in NPCE and of the electrode material matrix, respectively; C is the double layer capacitance (F cm^{-2}). The dimensionless time is expressed as:

$$\tau = \frac{\alpha C L^2(\kappa + \sigma)}{2\kappa\sigma} \tag{13}$$

where α is the transfer coefficient [5, 30].

The complex plane plots obtained for various EDLCs filled with different $TANBF_4$ salt solutions are given in Figs. 4 and 9 with the data fitted according to the SWM theory. For fitting of the Z'' vs. Z' plots, to a first approximation the high-frequency series resistance $R_s(\omega \to 0)$ and separator resistance R_{sep} have been fixed [30] according to the suggestion of the SWM theory [5]. As can be seen in Figs. 4 and 9, a very good agreement for all the electrolytes compared has been established, as a very small chi-squared function ($\chi^2 \leq 7\times10^{-4}$) and a weighted sum of squares ($\Delta^2 \leq 8\times10^{-2}$) [6, 7, 8, 30] have been obtained. The error bars of individual fitted parameters are shown in Figs. 10 and 11. According to the data in Fig. 10a, the effective conductivity, κ, for the electrolyte ions in the nanoporous matrix increases only very slightly with increasing ΔE, explained by the decrease of the series as well as parallel resistance values (R_s and R_p) with ΔE (i.e. with increasing the rate of the faradaic processes at higher ΔE values). At fixed ΔE, the effective conductivity of the electrolyte in the NPCE|PC solution capacitor increases in the order of the electrolytes as $Me_3EtN^+ < Me_2Et_2N^+ < MeEt_3N^+ \leq Et_4N^+ \leq Et_3PrN^+ < Et_3BuN^+$, i.e. with the increase of molar mass of the tetraalkylammonium cation used (Fig. 10a).

The effective conductivity of the electrode matrix, σ (Fig. 10b), depends on the electrolyte studied and σ increases in the same order of $TANBF_4$ solutions as κ, i.e. with increasing the effective conductivity of the electrolyte in the porous matrix. However, in comparison with the data in Fig. 10a, this dependency is very weak. Thus, there are small problems with the calculation (i.e. separation) of the values of σ and κ according to SWM theory [5] for the NPCE|PC + electrolyte interface because, to a first approximation, the effective conductivity of the electrode matrix has to be independent of the TAN^+ studied. Figure 11 demonstrates the dependence of the dimensionless time τ^* on the cell voltage ΔE for the cells filled with the different PC + $TANBF_4$ electrolytes. τ^* somewhat increases with ΔE and at ΔE = constant, τ^* increases with the molar volume of the cation investigated. Therefore the time needed for the penetration of the electrolyte ions through the electrolyte soaked in the nanoporous matrix increases with the molar mass of the electrolyte and, thus, with the decreasing the macroscopic molar conductivity of the electrolyte.

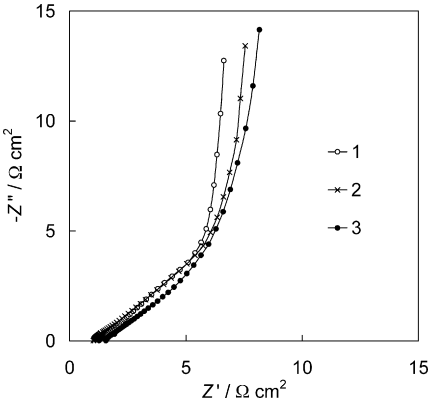

Fig. 9 Complex plane plots for the NPCE cell filled with 1 M solutions of $TANBF_4$ in PC for different electrolytes (*1*, Me_3EtNBF_4; *2*, Et_4NBF_4; *3*, Et_3BuNBF_4); *symbols*: experimental data; *solid lines*: fitting according to the Srinivasan and Weidner model [5, 30])

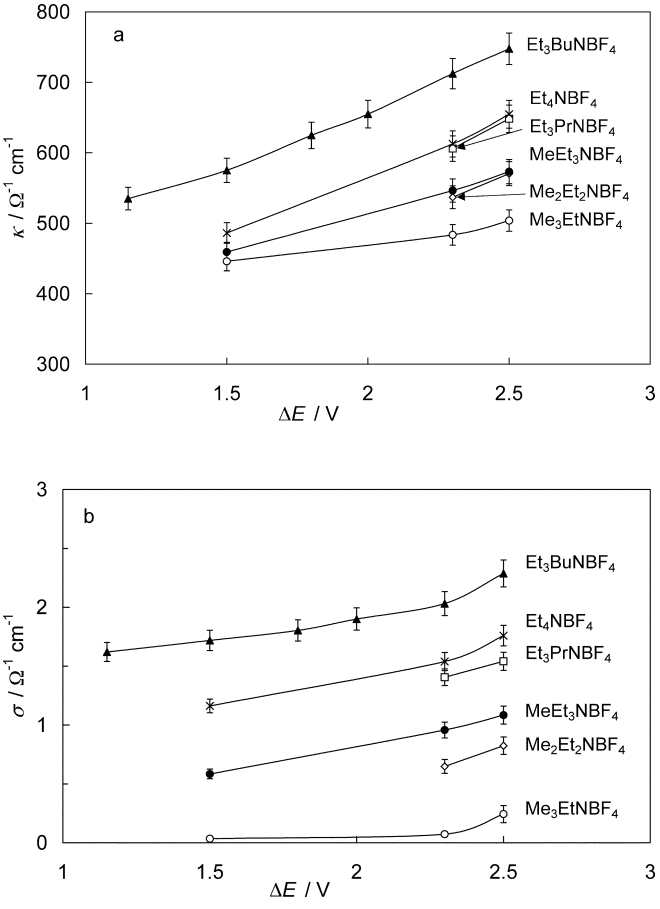

Fig. 10 Dependences of the effective conductivity of the electrolyte in the NPCE layer (**a**) and of the effective conductivity carbon matrix (**b**) on cell potential for the NPCE filled with 1 M solutions of different salts in PC, noted in the figure

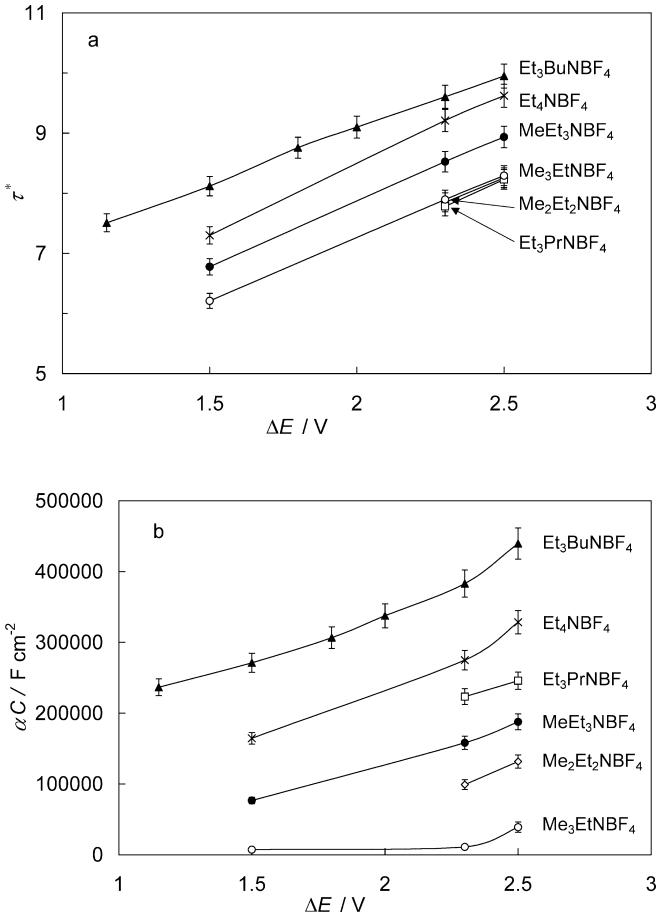

Fig. 11 Dimensionless time τ^* (**a**) and parameter αC (**b**) vs. cell potential dependences for the NPCE cell filled with 1 M solutions of different salts in PC, noted in the figure

From the results of simulations according to SWM theory [5, 30], the resistance of the separator R_{sep} very weakly increases with the molar mass of the TAN^+ cation in PC. Differently from AN and γ-BL systems [8], R_{sep} is practically independent of ΔE for the $PC + Me_3EtN^+$, $Me_2Et_2N^+$ and $MeEt_3N^+$ solutions. The effective conductivity of the electrolyte in a separator, κ_{sep}, decreases in the order AN > γ-BL > PC [8], but the dependence of R_{sep} on ΔE for PC solutions is comparatively small.

The data in Fig. 11b indicate that the parameter αC (where α is the transfer coefficient and C is the total capacitance) is very sensitive to the molar mass of the TAN^+ cation and the very high αC values for the $Et_3BuNBF_4 + PC$ solution indicate the noticeable adsorption of Et_3BuN^+ cations on the negatively charged electrode surface.

Conclusions

Electrical double layer capacitors based on two ideally polarizable nanoporous carbon electrodes in PC as the solvent for 1.0 M Me_3EtNBF_4, $Me_2Et_2NBF_4$, $MeEt_3NBF_4$, Et_4NBF_4, Et_3PrNBF_4 and Et_3BuNBF_4 electrolytes have been tested by cyclic voltammetry and electrochemical impedance methods. Using the impedance data it was found that the relaxation time constant, obtained from the relaxation frequency, is practically independent of the TAN^+ molar mass in the region of cell potential $\Delta E \le 2.0$ V. At $\Delta E > 2.0$ V, τ_R somewhat increases in the order of electrolytes $MeEt_3NBF_4 \le Me_2Et_2NBF_4 < Et_4NBF_4$, i.e. with increasing the electrolyte viscosity and decreasing the molar conductivity of solution. At very low frequency, $f < 0.01$ Hz, nearly equilibrium values of the series and parallel capacitances (C_s and C_p) have been established for the nanoporous carbon electrode (NPCE)|PC + $TANBF_4$ EDLC cells. However, the coincidence of the C_s and C_p values at $f < 0.005$ Hz, as well as the phase angle values $\delta \le -75°$ for NPCE|PC cells show, to a first approximation, that the adsorption equilibrium will be established only at very low frequencies.

The dependences of the normalized real and imaginary parts of the complex power versus frequency and phase angle versus frequency plots show that the relaxation time constant is independent of the TAN^+ cation characteristics and the low-frequency behaviour of the NPCE|PC + $TANBF_4$ cell is mainly determined by the solvent characteristics.

Analysis of the experimental data for various systems shows that the Srinivasan and Weidner model [5] can be used to fit the Nyquist plots measured at fixed ΔE. It was found that the effective conductivity for the electrolyte ions in the nanoporous matrix, κ, as well as the nanoporous carbon matrix conductivity, σ, increase with ΔE. The increase of κ and σ with ΔE can be explained by the migration of ions. Analysis of the impedance data indicates that the separator resistance increases somewhat with decreasing the molar conductivity of the electrolyte used in the electrical double layer capacitor.

Acknowledgements This work was supported in part by the Estonian Science Foundation under project no. 4568.

References

1. Conway BE (1999) Electrochemical supercapacitors: scientific fundamentals and technological applications, Kluwer/Plenum, New York
2. Pell WG, Conway BE, Marincic N (2000) J Electroanal Chem 491:9
3. Taberna PL, Simon P, Fauvargue JF (2003) J Electrochem Soc 150:A292
4. Salitra G, Soffer A, Eliad L, Cohen Y, Aurbach D (2000) J Electrochem Soc 146:2486
5. Srinivasan V, Weidner J (1999) J Electrochem Soc 146:1650
6. Lust E, Nurk G, Jänes A, Arulepp M, Nigu P, Permann L, Möller P (2002) Condens Matter Phys 5:307
7. Lust E, Nurk G, Jänes A, Arulepp M, Nigu P, Möller P, Kallip S, Sammelselg V (2003) J Solid State Electrochem 7:91
8. Lust E, Jänes A, Arulepp M (2004) J Electroanal Chem 562:33
9. Qu D, Shi H (1998) J Power Sources 74:99
10. Pell WG, Conway BE (2001) J Electroanal Chem 500:121

11. Christen Th, Carlen MW (2000) J Power Sources 91:210
12. Frichet A, Gimenez P, Keddam M (1993) Electrochim Acta 38:1957
13. Nishimo A (1996) J Power Sources 60:137
14. Burke A (2000) J Power Sources 91:37
15. Miller J (1998) Pulse power performance of electrochemical capacitors: technical status of present commercial devices. In: Proceedings of the 8th international seminar on double layer capacitors and similar energy storage devices, Deerfield Beach, Fla., USA
16. Vol'fkovich Yu M, Serdyuk T M (2002) Russ J Electrochem 38:1043
17. Maletin YA, Strizhakova NG, Izotov VY, Kozachkov SG, Mironova AA, Danilin VV (1996) Novel type of storage cells based on electrochemical double-layer capacitors. In: Barsukov V, Beck F (eds) New promising electrochemical systems for rechargeable batteries. Kluwer, Dordrecht, pp 363–372
18. Nurk G, Jänes A, Arulepp M, Nigu P, Permann L, Lust E (2001) Electric double layer structure at porous carbon electrodes. In: Meeting abstracts of the joint international meeting of ISE and ECS, San Francisco, abstr 1006
19. Leis J, Perkson A, Arulepp M, Käärik M, Svensson G (2000) Carbon 39:2043
20. Gregg SJ, Sing KSW (1982) Adsorption. Surface area and porosity. Academic Press, London, p 1
21. Macdonald JR, Johnson WB (1987) Fundamentals of impedance spectroscopy. In: Macdonald JR (ed) Impedance spectroscopy, Wiley, New York, pp 1–26
22. Roušar I, Micka K, Kimla A (1986) Electrochemical engineering, vol 2. Academia, Prague
23. Lust E, Jänes A, Lust K, Väärtnõu M (1997) Electrochim Acta 42:771
24. Frumkin AN, Melik-Gaikazyan VI (1951) Dokl Akad Nauk SSSR 77:855
25. Lorenz W (1958) Z Elektrochem 62:192
26. Armstrong RP, Rice WP, Thrisk HR (1968) J Electroanal Chem 16:517
27. Gileadi E (1993) Electrode kinetics for chemists, chemical engineering, materials scientists. VCH, New York, pp 291–305
28. Sluyters-Rehbach M, Sluyters JH (1970) Sine wave methods in the study of electrode processes. In: Bard A (ed) Electroanalytical chemistry, vol 4. Dekker, New York, pp 1–127
29. Cole KS, Cole RH (1941) J Chem Phys 9:341
30. ZView for Windows (version 2.7). Scribner, Southern Pines, NC, USA
31. de Levie R (1967) Electrochemical response of porous and rough electrodes. In: Delahay P, Tobias CW (eds) Advances in electrochemistry and electrochemical engineering, vol 6. Wiley-Interscience, New York, pp 329–397
32. Raistrick ID (1987) The electrical analogs of physical and chemical processes. In: Macdonald JR (ed) Impedance spectroscopy. Wiley, New York, pp 56–61
33. Ue M (1994) Electrochim Acta 39:2083
34. Gill DS (1977) Electrochim Acta 22:491